

The Falling Impact Analysis of Payload Cabin Carried by Aerostat in Near Space

Lulu Qian^{1,2,3,a}, Yixin Zhao^{1,2,b}, Guangming Wang^{1,2,c}, Zhanchao Wang^{1,2,3,d}, Wenhao Zhao^{1,2,e},
Jiang Wang^{1,2,f}, Min Huang^{*1,2,3,g1}

¹Key Laboratory of computational Optical Imaging Technology, China Academy of Sciences,
Beijing 100094;China

²Aerospace Information Research Institute, Chinese Academy of Sciences, Beijing 100094,China;

³University of Chinese Academy of Sciences, Beijing 10094.China

ABSTRACT

In order to investigate the payload cabin safety after falling impact in near space mission, based on the theory of nonlinear dynamics, the collision model of payload cabin is established by Ansys, and the Ls-Dyna analyzer is used for the simulation calculation to obtain the mechanical properties of buffer device during the impacting, and the structural mechanical response of the main structure of the load cabin. The result shows that the payload cabin impacts the ground with a speed of 7m/s and an acceleration of 3g which can meet the safety requirements. The cushioning effect of the buffer device can protect the payloads from the impact and is beneficial to recycle the internal devices. According to the recovery conditions of the payload cabin and internal devices after the falling impact experiments, the results are in good agreement with the conclusions obtained from the simulation analysis. The proposed simulation method is of great significance to the design and optimization of payload cabin in near space.

Key Words: Near Space; Payload Cabin; Nonlinear Dynamics; Impact Analysis; Buffer Device; Simulation Analysis.

1. INTRODUCTION

The near space generally refers to the altitude of 20~100 km at the airspace, which is a special position between aviation and aerospace [1]. The cabin is carried to the high-altitude in the near space to conduct scientific experiments. In order to ensure the follow-up processing of scientific experiments and to recycle the internal devices safely, a cutting knife which is in the load cabin will cut the cable when the scientific experiment is completed, subsequently the load cabin will deploy the parachute to return to the ground after it falls a certain distance. Considering that the impact at the moment of landing will cause severe damage to the structure of the load cabin. To recycle the devices in the payload cabin, it is necessary to conduct simulation analysis of the fall impact to optimize the payload cabin.

Direct at the requirements of the falling impact analysis of the payload cabin, this paper first briefly introduces the structure composition of the payload cabin, and the corresponding mechanical model is established using Ansys software. The Ls-Dyna solver is used to simulate the model, and during the impact, the mechanical characteristics of the buffer device and main structure of payload cabin are analyzed. The results of simulation analysis are in good agreement with the falling condition of the payload cabin after the scientific experiment.

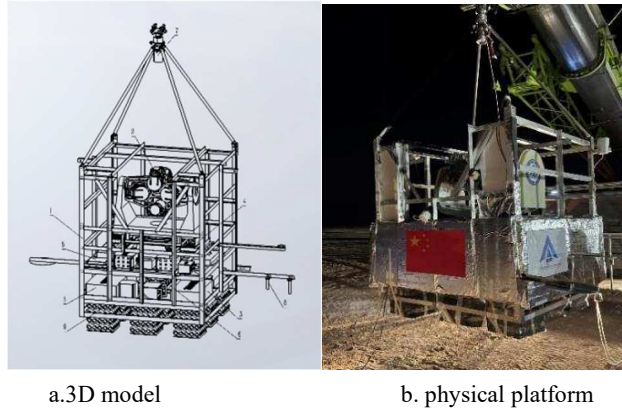
^{1a} qianll@aircas.ac.cn, ^b zhaoyx@aircas.ac.cn, ^c wanggm@aircas.ac.cn, ^d wangzhanchao@aoe.ac.cn, ^e zhaowh@aircas.ac.cn,

^f wangjiang@aircas.ac.cn, ^{*g} shuangmin@aircas.ac.cn

2. THE STRUCTURE DESIGN OF PAYLOAD CABIN

2.1 The structure of payload cabin

The payload cabin is mainly assembled by aluminum components with different sizes and shapes. It consists of observation camera system, energy battery, load control system, data transmission module, attitude control flywheel and other equipment. Outside the payload cabin there are reverse twist mechanism, measurement and control antenna, buffer device and polystyrene insulation board, as shown in Figure 1. To reduce the impact of the payload cabin when it lands, nine buffer devices are installed in the bottom of the cabin to ensure that the instruments and equipment can be safely recovered. To figure out the buffer ability during landing impact, the mechanical properties of the buffer device are analyzed.



1-payload cabin, 2-observation camera system, 3-energy battery, 4-load control system, 5- data transmission module, 6- attitude control flywheel, 7-reverse twist mechanism, 8- measurement and control antenna, 9-buffer device

Figure.1 The model of payload cabin

2.2 The structural model of buffer device

The payload cabin has built-in scientific instruments and equipment, and returns to land after data collection and transmission in the near space. At this time, the payload cabin carrying valuable scientific instruments and experimental data that have been stored but cannot be transmitted in real time is desirable to land safely.

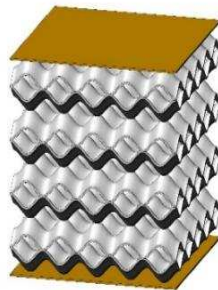


Figure.2 The model of buffer device

Considering the structure quality, landing attitude and economic feasibility of the payload cabin, the buffer device is made of pulp egg tray by forward and reverse bonding. The buffer device is attached to the bottom of the cabin body. During the impact process of the payload cabin landing, the buffer device will absorb energy through compression deformation, reducing the impact on the payload cabin, thus playing an important role in protecting the instruments and equipment in the cabin. The buffer device is shown in Figure 2.

3. SIMULATION ANALYSIS OF THE PAYLOAD CABIN FALLING IMPACT PROCESS

3.1 Impact process and simulation assumptions

The simulation process is divided into two stages. Firstly, from the moment when the buffer device touches the ground, it is compressed by the payload cabin, during which part of the buffer device will be peeling off and crushed due to direct failure of absorbing impact energy. In this process, the buffer device is the major subject of impact. According to Newton's third law, the force constraint of the contact surface is[4]:

$$\begin{cases} t_N^{buffer} + t_N^{ground} = 0 \\ \tau_N^{buffer} + \tau_N^{ground} = 0 \end{cases} \quad (1)$$

where t_N^{buffer} is the normal contact force of the buffer device; t_N^{ground} is the normal contact force of the ground; τ_N^{buffer} is the tangential contact force of the buffer device, τ_N^{ground} is the tangential contact force of the ground.

After the payload cabin is in contact with ground, the buffer device loses its buffering effect, and the payload cabin becomes the main subject of impact, which is the second stage, and the force equation of the contact surface is changed to:

$$\begin{cases} t_N^{cabin} + t_N^{ground} = 0 \\ \tau_N^{cabin} + \tau_N^{ground} = 0 \end{cases} \quad (2)$$

where t_N^{cabin} and τ_N^{cabin} are the normal contact force and tangential contact force of the payload cabin, respectively.

During the whole landing process, there are many complicated influencing factors. In order to highlight the buffering effect of the pulp egg tray, we made some approximate treatment for the buffering process [3]: considering the duration of landing buffer process is short, the heat exchange can be neglect, thus, the compression of buffer device is assumed to be an adiabatic compression process.

3.2 The finite element discrete simulation method

Discretize the structure of the payload cabin and buffer device, the spatial coordinate $x_i(X, t)$ of any particle $X_{cabin,buffer}$ on the element at any time is:

$$x_i(X, t) = N_I x_{iI}(t) \quad i = 1, 2, 3 \quad (3)$$

where N_I is the Lagrange interpolation function of the node I on the element. $x_{iI}(t)$ is the coordinate value of node I in the direction I of the element at time t .

Consequently, the displacement of any point X in the element can be obtained as:

$$\mu_i(X, t) = x_i(X, t) - X_i = N_I(X) \mu_{iI}(t) \quad (4)$$

where $\mu_{iI} = x_{iI}(t) - X_{iI}$ is the displacement of node I in the element. In a similar way, the velocity, acceleration, deformation rate and imaginary velocity at any point in the element can be expressed as:

$$\begin{cases} \dot{\mu}_i(X, t) = N_I(X) \dot{\mu}_{iI}(t) \\ \ddot{\mu}_i(X, t) = N_I(X) \ddot{\mu}_{iI}(t) \\ D_{ij} = \frac{1}{2} \left(\frac{\partial \dot{\mu}_i}{\partial x_j} + \frac{\partial \dot{\mu}_j}{\partial x_i} \right) = \frac{1}{2} \left(\dot{\mu}_{iI} \frac{\partial N_I}{\partial x_j} + \dot{\mu}_{jI} \frac{\partial N_I}{\partial x_i} \right) = B_I \mu_I \\ \delta v_i(x) = N_I(x) \delta v_{iI} \end{cases} \quad (5)$$

Substitute the above formulas into the imaginary power equation:

$$\int_V \frac{\partial(\delta v_i)}{\partial x_j} \sigma_{ij} dV - \int_V \delta v_i \rho b_i dV - \int_{A_1} \delta v_i \bar{t}_i dA + \int_V \delta v_i \rho \ddot{\mu}_i dV = 0 \quad (6)$$

where V is present time construction; v_i is instantaneous velocity of a particle; x_i is the coordinate of the particle in this moment; $\frac{\partial v_i}{\partial x_j}$ is the velocity gradient tensor; σ_{ij} is the Cauchy stress; ρ is the density of present time construction; b_i

is the force acting on the object unit mass; A_1 is the impact contact area; \bar{t}_i is mean surface force; $\ddot{\mu}_i$ is the particle acceleration.

After sort out:

$$M\ddot{U} + f^{int} = f^{ext} \quad (7)$$

where

$$f^{int} = \int_V B^T \sigma dV \quad (8)$$

$$f^{ext} = \int_V N^T \rho b dV + \int_{A_1} N \bar{t} dA \quad (9)$$

$$M = \int_{V_0} \rho N^T N dV_0 \quad (10)$$

M is the system mass matrix, it's not about time, just at the initial moment calculation.

4. FINITE ELEMENT MODELING

4.1 Model simplification

To simplify the calculation model and improve the calculation efficiency, the structure of the payload cabin is simplified. Preserving the cabin structure, the complex load distribution is replaced by equivalent mass center. The model framework connecting holes are also filled to reduce the simulation time and to ensure the operation model of inertial characteristics without affecting the accuracy of the calculation results.

4.2 Material setup

The cabin frame material is 2A12, and the material constitutive model is chosen as Johnson Cook. The buffer device material is pulp, and the Plastic Kinematic model is selected. The material parameters are shown in the following table:

Table.1 material characteristic parameter table[5],[6]

2A12	A/Mpa	B/Mpa	n	C	m
	396	540	0.41	0	1
	D ₁	D ₂	D ₃	D ₄	D ₅
	0.22	0.12	2.8	0	0
Pulp	A/Mpa	E/Mpa	ν	T/Mpa	$\rho/\text{kg/m}^3$
	6.9	12.26	0.38	4.765	1200

4.3 Boundary conditions

Through analysis of previous experimental data, the speed of the payload cabin is about 7m/s[7] and the acceleration is about 3g when it reaches the ground. In order to simplify the calculation process, the boundary conditions for the fall impact analysis of the payload cabin can be set as following: the overall initial velocity of the payload cabin is 7m/s and the acceleration is 3g; the fall impact is carried out at an angle of 15° with the horizontal plane at a height of 10mm above the ground, as shown in Fig 3.

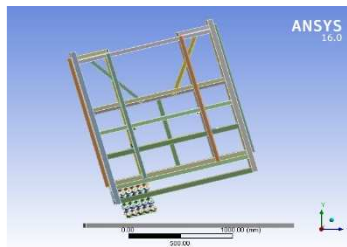


Figure.3 The model of boundary conditions

5. ANALYSIS OF SIMULATION RESULTS

5.1 Strain and stress analysis of the buffer device

The analysis time is set as 0.05s. Three moments were selected to check the stress results, namely, the moment when the buffer device touched the ground, the middle of impact process and the moment when the analysis ended. The stress contour figure is shown as the following:

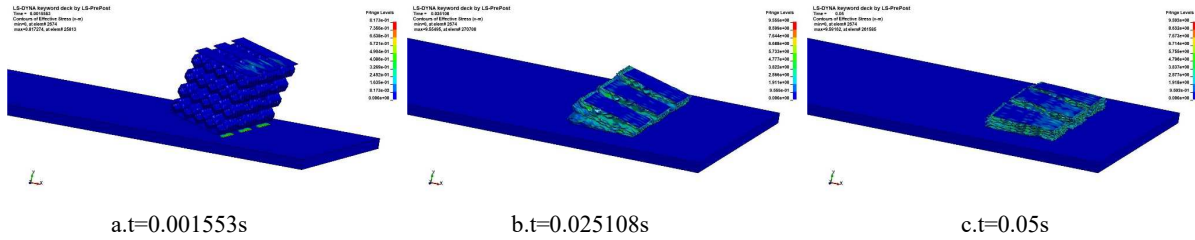


Figure.4 Stress contour figure of buffer device during landing cushioning process

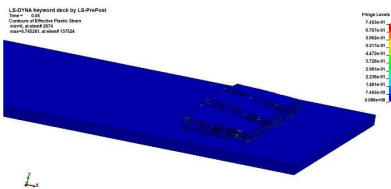
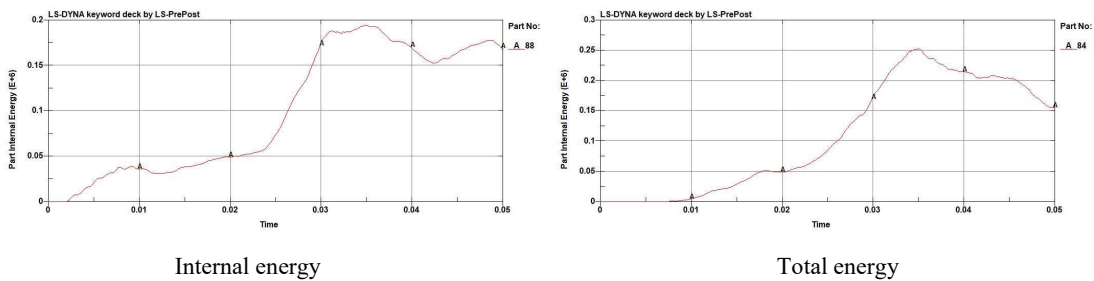


Figure.4 Strain of the buffer device

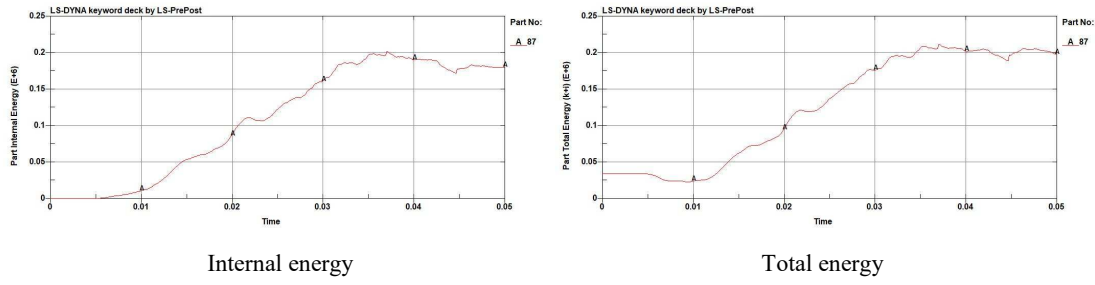
As can be seen from FIG. 4 and 5, the stress change of the buffer device during the landing process of 0.05s reached 9.555MPa in the middle part of the analysis time, exceeding the initial yield strength of the material. The maximum plastic strain was 0.7453, which did not exceed the initial failure strain 0.8 set by the analysis, indicating that during the landing process the buffer device works well in cushioning and absorbing energy. When the frame of the payload cabin touches the ground, the force body changes, and the frame absorbs most of rest energy, and the buffer device always play a certain role in the landing process.

5.2 Internal and total energy analysis

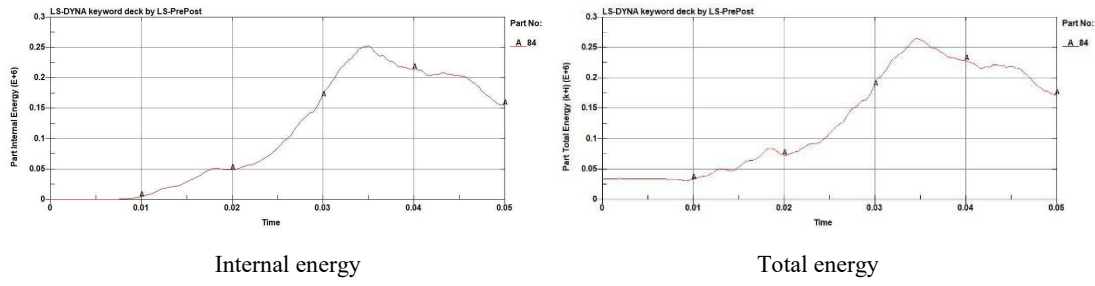
Three parts of the bottom, middle and upper layers of the buffer device were selected to analyze the internal and total energy results during landing, as shown in the following figure:



a. The internal and total energy of bottom part



b. The internal of middle part



c. The internal of top part

Figure.5 The different layer internal of buffer device

As can be seen from Figure 6, the maximum energy absorbed by each layer of the buffer device during landing is about 200J, accounting for more than 90% of the total energy at the same time, and the absorption energy is sufficient to play a buffer role.

5.3 Strain and stress analysis of the payload cabin

Three moments were selected to check the stress results, namely, the moment when the payload cabin touched the ground, the middle of impact process and the moment when the analysis ended. The stress contour figure is shown as following:

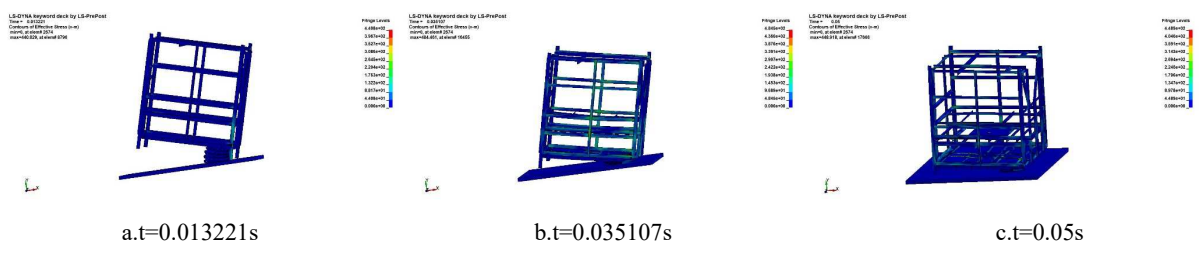


Figure.6 Stress contour figure of payload cabin during landing cushioning process

As can be seen from Figure 6, the stress change of the payload cabin body during the landing process of 0.05s shows that the stress of the payload cabin body at the moment of contact with the ground has reached 440.8MPa; when $t=0.05s$, the stress of the payload cabin body is about 448.9MPa. During the landing process, it can be seen that some units have failed and dropped, but the main body of the payload cabin is not seriously damaged during the landing process.

5.4 Comparison of experimental results

As shown in the figure, most of the buffer devices are deformed and damaged by compression and shear, but the whole frame of the cabin is complete. In addition to the large deformation of the bottom beam at the bottom of the cabin structure, the rest of the deformation is small, and all the equipment is safely recovered.



Figure.7 Photographs of the payload cabin after landing

6. CONCLUSION

In this paper, a falling impact model of the payload cabin is established, and the landing process of the cabin body under the conditions with specific angle, initial velocity and acceleration is simulated by Ansys/LS-Dyna software. The stress-strain contour figure, internal energy and total energy curves of the buffer device under the landing buffer change over time are obtained[8]. The maximum stress and strain values of the buffering device are obtained, and the energy situation and the buffering performance are analyzed. Despite the bottom part of the beam is damaged, in the impact process, the main frame of the cabin body has a small force and a complete structure, indicating that the buffer device can withstand a large impact, good energy absorption effect, and has a good dynamic buffer characteristics. The landing buffer is an overly complicated process. In this paper, only the case of 15° deviation from the vertical axis is studied, and the ground is assumed to be rigid. The modeling of the ground and landing attitude information of the capsule will be the focus of future research.

7. ACKNOWLEDGEMENT

This research was funded by the civil space debris project (Grant NO: KJSP2020020201) and Youth Innovation Promotion Association CAS.

8. REFERENCES

- [1] Tong Jing-yu, Xiang Shu-hong. Near space environment and environment tests[J]. Equipment Environment Engineering,2012,9(3):1-4.
- [2] Yuan Pei-yin, Zhao Yu, Lei Lin, et al. Simulation analysis of dynamic characteristics of collision between ship and dock based on LS-DYNA[J]. Ship Science and Technology,2021,3(3):29-32
- [3] Bai Jin-ze. Ls-DYNA theoretical basis and case study[M]. Beijing: Science Press,2005.
- [4] Yi Jing-qiang, Hao Gui-xiang, Wang Hong-yan, et al. Cushioning Process Study on Airbag System of On-plateau-airdropped Equipments[J]. Chinese Journal of Construction Machinery,2012,10(3):364-368.
- [5] Yan Yi-xia, et al. Numerical Simulation for Drop Test of the Conical Shell[C]. The 10th National Symposium on Impact Dynamics.2011.
- [6] Matthew A Barsotti, John M H Puryear, David J. Stevens. Modeling Mine Blast with SPH[C]. 12th International LS-Dyna Conference, Detroit,2012.
- [7] Tian Chun-min, Huang Min, Qian Lu-lu. Dynamics Analysis of Load Cabin Carried by High-Altitude Balloons in Near Space[J]. Machinery Design & Manufacture, 2020,12(12);205-207.
- [8] Li Liang-chun, Huang Gang, et al. Simulation Analysis of New Type Landing Cushion Airbag Based on ANSYS/LS-DYNA[J]. Packing Engineering, 2012,8(15):16-20.